UDC 004.93

MACHINE LEARNING FOR AUTOMATIC EXTRACTION OF WATER BODIES USING SENTINEL-2 IMAGERY

Kashtan V. Yu. – PhD, Associate Professor, Associate Professor of Department of Information Technology and Computer Engineering, Dnipro University of Technology, Dnipro, Ukraine.

Hnatushenko V. V. – Dr. Sc., Professor, Head of Department of Information Technology and Computer Engineering, Dnipro University of Technology, Dnipro, Ukraine.

ABSTRACT

Context. Given the aggravation of environmental and water problems, there is a need to improve automated methods for extracting and monitoring water bodies in urban ecosystems. The problem of efficient and automated extraction of water bodies is becoming relevant given the large amount of data obtained from satellite systems. The object of study is water bodies that are automatically extracted from Sentinel-2 optical satellite images using machine learning methods.

Objective. The goal of the work is to improve the efficiency of the process of extracting the boundaries of water bodies on digital optical satellite images by using machine learning methods.

Method. The paper proposes an automated information technology for delineating the boundaries of water bodies on Sentinel-2 digital optical satellite images. The process includes eight stages, starting with data download and using topographic maps to obtain basic information about the study area. Then, the process involved data pre-processing, which included calibrating the images, removing atmospheric noise, and enhancing contrast. Next, the EfficientNet-B0 architecture is applied to identify water features, facilitating optimal network width scaling, depth, and image resolution. ResNet blocks compress and expand channels. It allows for optimal connectivity of large-scale and multi-channel links across layers. After that, the Regional Proposal Network defines regions of interest (ROI), and ROI alignment ensures data homogeneity. The Fully connected layer helps in segmenting the regions, and the Fully connected network creates binary masks for accurate identification of water bodies. The final step of the method is to analyze spatial and temporal changes in the images to identify differences, changes, and trends that may indicate specific phenomena or events. This approach allows automating and accurately identifying water features on satellite images using machine learning.

Results. The implementation of the proposed technology is development through Python software development. An assessment of the technology's accuracy, conducted through a comparative analysis with existing methods, such as water indices and K-means, confirms a high level of accuracy in the period from 2017 to 2023 (up to 98%). The Kappa coefficient, which considers the degree of consistency between the actual and predicted classification, confirms the stability and reliability of our approach, reaching a value of 0.96.

Conclusions. The experiments confirm the effectiveness of the proposed automated information technology and allow us to recommend it for use in studies of changes in coastal areas, decision-making in the field of coastal resource management, and land use. Prospects for further research may include new methods that seasonal changes and provide robustness in the selection and mapping of water surfaces.

KEYWORDS: extraction, water bodies, optical satellite images, water spectral indices, machine learning, Kappa coefficient, Pearson coefficient, confusion matrix.

ABBREVIATIONS

OLI is an Operational Land Imager;
ETM is an Enhanced Thematic Mapper Plus;
CNNs are Convolutional Neural Networks;
ResNet is a Residual neural network;
ReLU is a rectified linear unit;
ROI is a Region of Interest;
RPN is a Regional Proposal Network;
FCN is a fully connected network;
TP is a True Positive;
TN is a True Negatives;
FP is a False Positive;
FN is a False Negatives;
IR is the infrared channel;
RMSE is a Root Mean Square Error;
PDF is a Probability Density Function;
OA is an Overall Accuracy;
NDSI is a Normalized Difference Snow Index;
NDWI is a Normalized Difference Water Index;
MNDWI is a Modified Normalized Difference Water Index;
XGBoost is an eXtreme Gradient Boosting.

NOMENCLATURE

L_{λ} is an energy brightness for the spectral zone [W/(s ⩾2 nm)];
D is an distance from the Earth to the Sun in astronomical units for a particular period;
$E_{sun\lambda}$ is an average solar extraterrestrial irradiance [W/(m2 nm)];
θ is an angle of the Sun;
x' is an input; x is the output;
y is an final output;
L is an length of the coastline;
W is an width of the coastline;
$\bar{x}$, $\bar{y}$ are average values of two variables x and y, respectively;
T is a total number of pixels in the Sentinel-2 image;
L is a length of the coastline;
W is a width of the coastline.

DOI 10.15588/1607-3274-2024-1-11

INTRODUCTION

Water is an inexhaustible source of life and a critical element for urbanized ecosystems. The impacts of human exploitation, land use change, land disturbance, and climate change are hurting the hydrological cycle. These factors lead to a restructuring of the distribution of surface and groundwater on our planet [1].

The growing impact of global climate change and intense human activity is leading to significant changes like rivers: shrinking wetlands increased flooding, and other changes in the spatial and temporal distribution of water resources. Despite these transformations, the dynamics of changes in surface water bodies remain poorly understood, especially in the context of their seasonal and interannual characteristics. The lack of information in this context makes it difficult to fully understand the patterns that govern the dynamics of water bodies [2].

Given the importance of this issue, real-time access to information on the spatial distribution and changes over time of wetlands, estuaries, and river floods appears to be fundamental to understanding the interaction of regional hydrology and climate change, as well as to the effective management of surface water resources [3]. In this context, remote sensing is coming to the forefront as an effective means of monitoring changes in surface water bodies in real-time and providing dynamic access to information about the earth's surface [4].

The object of study is the water surfaces of urban ecosystems that are automatically extracted from Sentinel-2 optical satellite images using machine learning methods.

The subject of study is the extraction of water bodies technology on digital optical satellite images using machine learning methods.

The purpose of the work is to enhance the efficiency of detecting water body boundaries on digital optical satellite images using machine learning methods.

1 PROBLEM STATEMENT

Data obtained from space satellites such as Landsat, Advanced Spaceborne Thermal Emission and Reflection Radiometer, Satellite Pour l'Observation de la Terre, and Sentinel-1 and Sentinel-2 open up opportunities for a wide range of applications. These data allow for flood monitoring, water resource assessment [5], water quality [6], and coastal monitoring [7]. These products play a crucial role in contemporary approaches to monitoring and managing water resources and the natural environment. Nevertheless, optical satellite images may include clouds, as noted by [8], along with their shadows, posing challenges in processing such data and identifying water features. Special emphasis needs to be placed on investigating coastal ecotone zones, distinctive regions where a transitional zone emerges between land and water, frequently characterized by aquatic vegetation. These ecotones significantly influence the precision of identifying and classifying water bodies in satellite imagery.

Thus, optical satellite images can provide information for monitoring water bodies. On the other hand, given the difficulties associated with cloud shadows and low-albedo objects, it is necessary to continuously improve methods for recognizing water features on satellite images.

2 REVIEW OF THE LITERATURE

Currently, there are developed methods for detecting, mapping, and monitoring water bodies on satellite images. These methods can be divided into three main groups: pixel-based statistical pattern recognition analysis, which includes supervised [9] and unsupervised [10] classification approaches; image analysis, taking into account parameters such as spectral characteristics, texture, shape complexity [11] and sub-pixel analysis [12]. Water spectral indices are widely used for monitoring water bodies. The researchers compared the effectiveness of different water indices in Landsat 7 ETM+, Landsat 8 OLI, and Sentinel-2 MSI. The study [13] proposed a new water index for Landsat Thematic Mapper /Enhanced Thematic Mapper Plus (ETM+)/OLI satellites based on surface reflectance using a threshold value. This method is optimized for processing large amounts of data and provides a simple but effective approach for the automated classification of large water bodies by area. Although existing methods based on water spectral indices can provide high accuracy in determining surface water areas, they are ineffective when analyzing multispectral satellite images.

Classification methods that use feature extraction and machine learning are advanced techniques for monitoring surface water bodies, such as random forests [14], support vector machines [15], and XGBoost [16]. On the other hand, unsupervised classification methods do not require training samples and are more suitable for developing automated algorithms. CNNs are considered a popular deep learning method and are commonly used for semantic segmentation, cloud detection, water feature extraction, and other tasks [17]. A lot of new deep-learning models have been developed for surface water body extraction based on satellite data [18], for which multiscale semantic information is important.

3 MATERIALS AND METHODS

The extraction of water bodies technology proposed in this paper consists of eight stages, as shown in Figure 1.

The first stage consists of downloading images from 2017 to 2023 from the Sentinel-2 optical satellite in the summer. Then use the topographic maps that contain basic information about the study area. To map the contours of water bodies on topographic maps, we use geospatial analysis to determine the coordinates of the coastline on the map.

The second stage is data pre-processing, which includes calibration of satellite images, removal of atmospheric noise, and contrast enhancement. The task of radiometric calibration is to convert brightness values (Digital Number) into spectral energy brightness values at the upper atmosphere boundary.

DOI 10.15588/1607-3274-2024-1-11

The transmission of electromagnetic radiation and the atmosphere's glow were taken into account for atmospheric correction. At the same stage, pixel values were converted from energy brightness to reflectance coefficients from 0 to 1 [19]:

$$p_{\lambda} = \frac{\pi \times L_{\lambda} \times D^2}{E_{sun\lambda} \times \cos\theta}, \qquad (1)$$

where L_{λ} is the energy brightness for the spectral zone [W/(s ⩾2 nm)]; D is the distance from the Earth to the Sun in astronomical units for a particular period; $E_{sun\lambda}$ is the average solar extraterrestrial irradiance [W/(m2 nm)]; θ is the angle of the *Sun*.

To use the EfficientNet-B0 architecture to identify water bodies. The EfficientNet architecture defines an efficient approach to image processing developed using the AutoML method [19]. The main idea behind this architecture is to optimally scale the network width, network depth, and image resolution.

EfficientNet consists of 8 variations, designated from B0 to B7, each with its number of parameters and accuracy. This series of architectures is designed with limited resources in mind, and B0 is the lightest version suitable for use in resource-constrained applications.

Depth convolution is performed independently for each input channel, which is a spatial convolution [20]:

$$x' = \mathrm{DepthwiseConv}(x), \qquad (2)$$

where x' is the input; x is the output; DepthwiseConv uses spatial convolution for each channel independently.

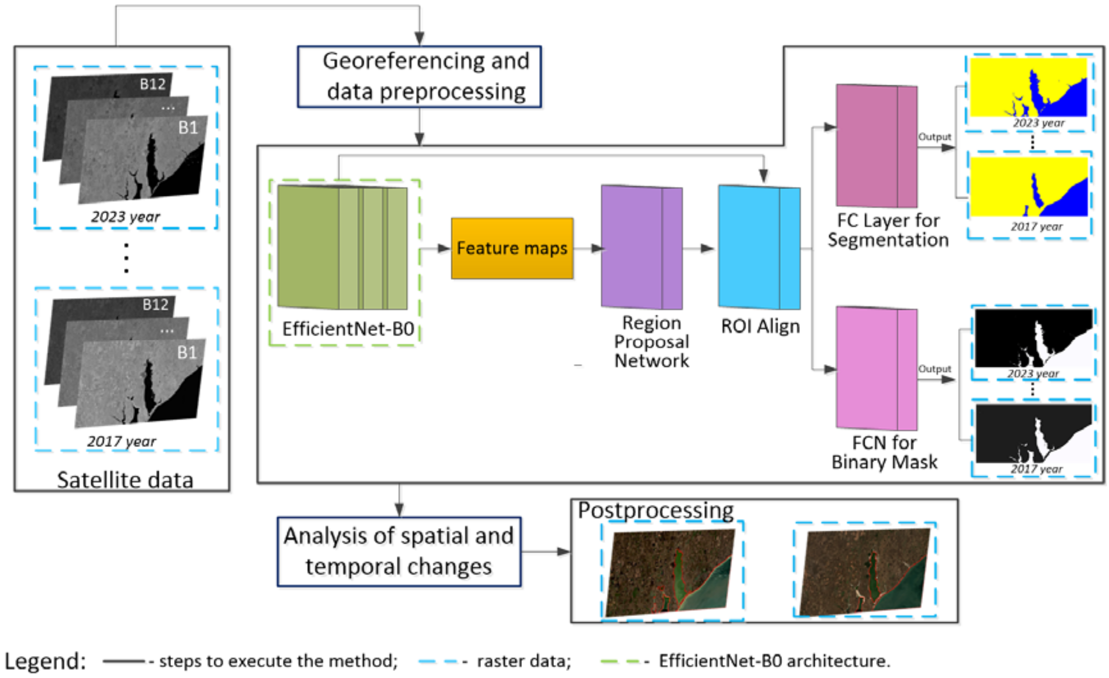

Figure 1 – Algorithm of the proposed technology

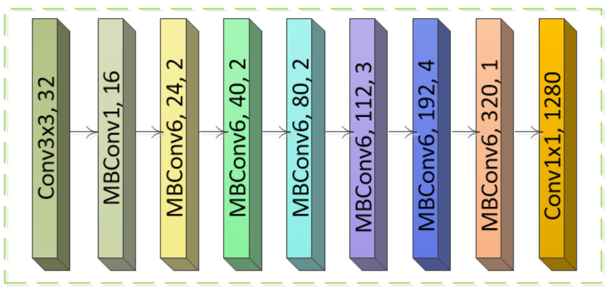

Figure 2 – EfficientNet-B0 architecture

Point convolution projects the channel output resulting from depth convolution onto a new channel space using a 1×1 convolution [20]:

$$y = \mathrm{PointwiswConv}(x'), \qquad (3)$$

where y is the final output.

ResNet blocks consist of a layer that compresses the channels and a layer that expands the channels. This allows bandwidth-intensive connections to be linked to channel-rich connections in layers. Linear activation is used in the last layer of each block to prevent loss of information from the ReLU [21].

In the next stage, using the output data from EfficientNet-B0, feature maps are created for further use. These feature maps contain important information features of the image that will be used in the analysis and processing. The Regional Proposal Network is used to determine the ROI. The RPN is responsible for identifying potential locations where objects may be located. The ROI alignment process is performed to ensure data homogeneity. It may include resampling or other operations to bring all ROIs to the same standard size or format. A fully

DOI 10.15588/1607-3274-2024-1-11

connected layer is used to segment the ROIs. This layer helps to divide the image into different classes or areas that are important for further analysis. A FCN is used to create binary masks. These masks identify areas that have water features.

The final stage of the algorithm is the analysis of spatial and temporal changes in the images. It includes identifying differences, changes, and trends in the images that may indicate certain phenomena or events.

4 EXPERIMENTS

This paper tested the proposed information technology on the example of the Molochnyi Lyman, located in the south of Zaporizhzhia Oblast within the Melitopol district, which is an arid region of southern Ukraine, where high temperatures are observed, especially in recent years, due to global warming. Such climatic conditions cause increased evaporation from its water surface up to 155 million m³ per year, sometimes even up to 250 million m³.

Figure 3 – Study area

The Pearson's *r* coefficient was used to analyze the change in the area of the Molochny Lyman water mirror [22]:

$$r = \frac{\sum(x-\bar{x})(y-\bar{y})}{\sum(x-\bar{x})^2(y-\bar{y})^2}, \quad (4)$$

where $\bar{x}$, $\bar{y}$ are the average values of two variables *x* and *y*, respectively.

Two metrics were calculated to assess the effectiveness of the water body monitoring technology proposed in this paper: OA and Kappa coefficient. These metrics provide an objective assessment and compare the effectiveness of the developed method with water indices and the K-means method [22]:

$$OA = \frac{TP+TN}{T}, \quad (5)$$

$$Kappa = \frac{T\times(TP+TN)-(TP+TN)}{T\times T-(TP+TN)}, \quad (6)$$

where *T* is the total number of pixels in the Sentinel-2 image; *TP*, *TN* are the categorized pixels by comparing the extracted water pixels with the reference map: *TP* are true positives, i.e., the number of correctly extracted pixels; *TN* is the number of correctly identified pixels that are not water bodies and were correctly categorized into another class.

Confusion Matrix (Fig. 4) is an important tool for evaluating the effectiveness of classification models in machine learning and computer vision tasks. This tool allows you to visualize the classification results and determine the accuracy level of the model. The matrix determines the number of objects that were correctly or incorrectly classified in each category: TP is the number of correctly identified positive classes. TN is the number of correctly identified negative classes. FP is the number of false positive classes. FN is the number of false negatives identified. It is a useful tool for understanding the types of errors that can occur during classification [22].

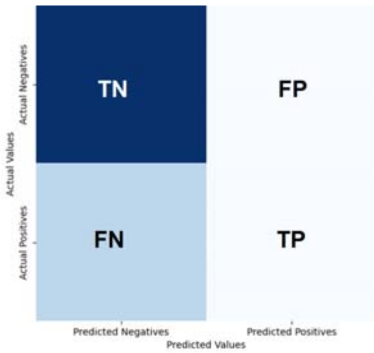

Figure 4 – Graphical presentation of Confusion Matrix

5 RESULTS

The Pearson correlation coefficient was used to assess changes in water bodies and the coastline, which can have a value ranging from -1 to 1. A value close to 1 indicates a strong positive relationship between the masks, a value close to -1 indicates a strong negative relationship and a value close to 0 indicates no relationship. The results of the Pearson's coefficient values are shown in the form of a graph in Fig. 5.

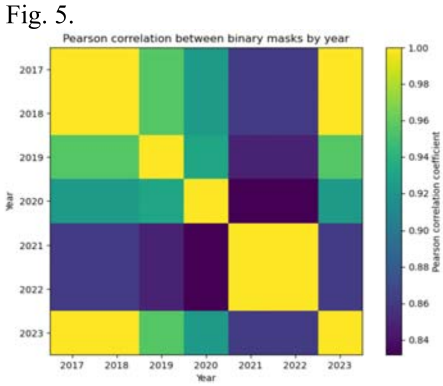

Figure 5 – Graph of Pearson's coefficient values by year

DOI 10.15588/1607-3274-2024-1-11

The resulting water body contours were analyzed in detail using geographic information technologies and the Python programming language (Fig. 6). The analysis of water body contours made it possible to determine the nature of changes, their intensity, and distribution along the coastal zone of the Molochny Lyman.

The next step is to analyze the average annual rate of change in the area of water bodies of the Molochny Lyman between 2017 and 2023. At this stage, the water mirror area was calculated, as well as the nature of the changes, their intensity, and distribution along the coastal zone of the Molochny Lyman for 6 years:

$$S = L \times W, \qquad (7)$$

where L is the length of the coastline; W is the width of the coastline.

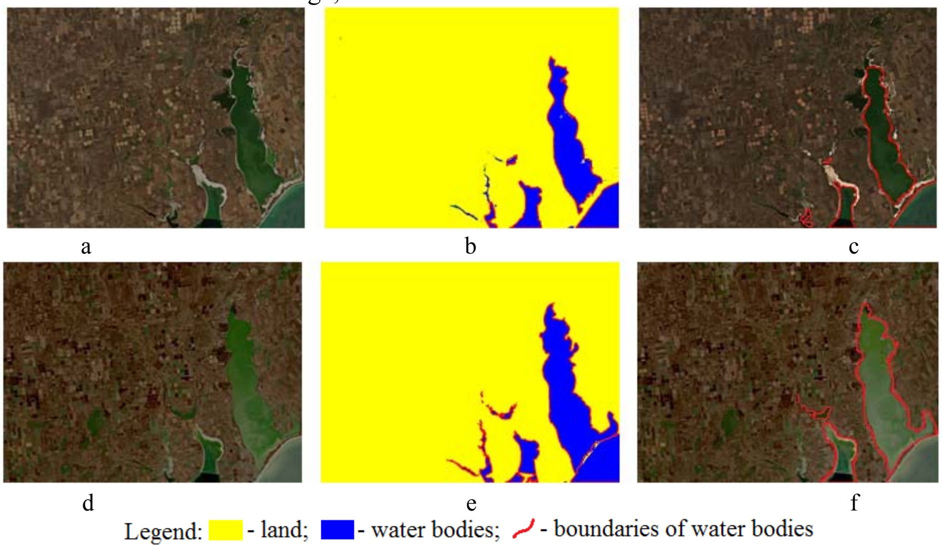

Figure 6 – The result of the proposed technology: a – Satellite image of 2017; b – selection of water bodies after segmentation in 2017; c – automated selection of water bodies on the satellite image of 2017; d – Satellite image of 2023; e – selection of water bodies after segmentation in 2023; f – automated selection of water bodies on the satellite image of 2023

Figure 7 shows a graph of changes in the water surface area of the Molochny Lyman from 2017 to 2023 years.

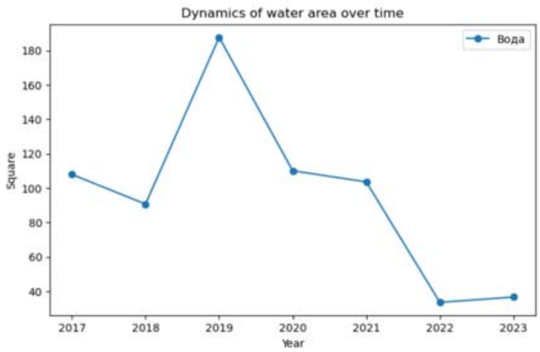

Figure 7 – Graph of changes in the area of the water mirror of the Molochny Lyman

In this study, a graph of the values of the coastal zone reflection coefficients in the IR channel for the period 2017–2023 was constructed and analyzed (Fig. 8). Changes in the values of the reflection coefficients in the IR channel indicate differences in the temperature and heat transfer of the coastal zone. It may be due to climate change, expansion or contraction of water bodies, or other natural and anthropogenic impacts.

In 2019, we took large-scale measures to restore the relationship between the Molochnyi Lyman and the Sea of Azov during the information verification. In particular, on December 27, 2019, the estuary began to be filled with seawater, which led to a rise in water level and a decrease in water salinity in some places to 25 ppm. These actions have become a significant factor that may affect the water area in the estuary and its ecosystem in the future.

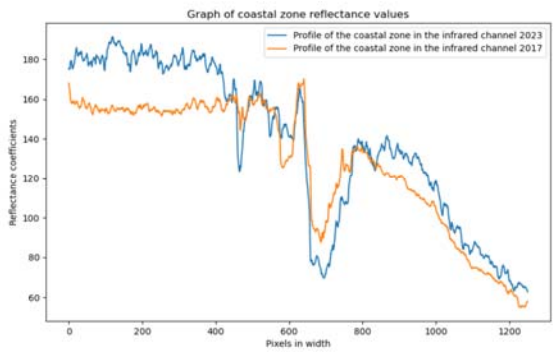

Figure 8 – Graph of coastal zone reflection coefficients in the infrared channel

Table 1 shows the results of the OA and Kappa metrics for the proposed technology and the NDWI, MNDWI [23], and K-means indices. In 2017 and 2023, the proposed technology identifies water bodies with an accuracy of 98% and a Kappa coefficient of 0.96. Compared to this, other methods, such as NDWI, MNDWI, and K-means have lower performance.

DOI 10.15588/1607-3274-2024-1-11

Table 1 – Results of the water body contouring accuracy assessment

Methods	2017 year		2023 year	
	OA	Kappa	OA	Kappa
NDWI	77%	0.64	77%	0.51
MNDWI	90%	0.82	93%	0.86
K-means	95%	0.88	94%	0.86
Proposed technology	98%	0.96	98%	0.96

Root Mean Square Error is used to evaluate the accuracy of a technology by comparing its predicted values to the actual values [24, 25]. A low RMSE value indicates the technology has high accuracy, while a high value may indicate low accuracy. To summarize the information according to Fig. 9, the low RMSE value for the proposed method indicates its high accuracy compared to other methods, and the high value for the NDSI method indicates a significant difference between predicted and actual values and the need for further optimization and refinement of the technology.

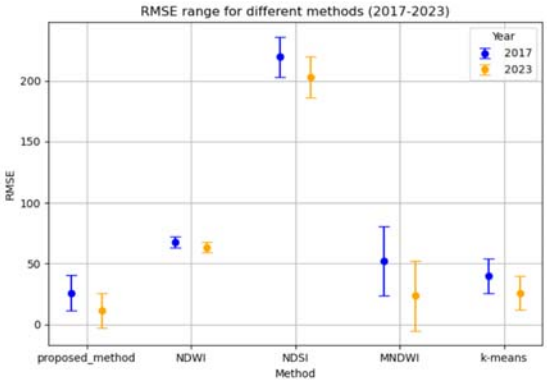

Figure 9 – RMSE value graph

The histogram in Fig. 10 of the probability density function of the coastal zone, with the highlighting of land, water, and Otsu threshold pixels, provides information about the distribution of areas in the image.

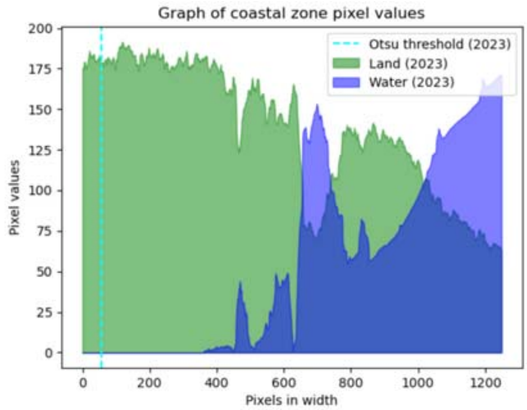

Figure 10 – Histogram of the PDF

The Confusion matrix (Fig. 11) displays the results of the classification models, showing the number of correctly and incorrectly classified objects in each category.

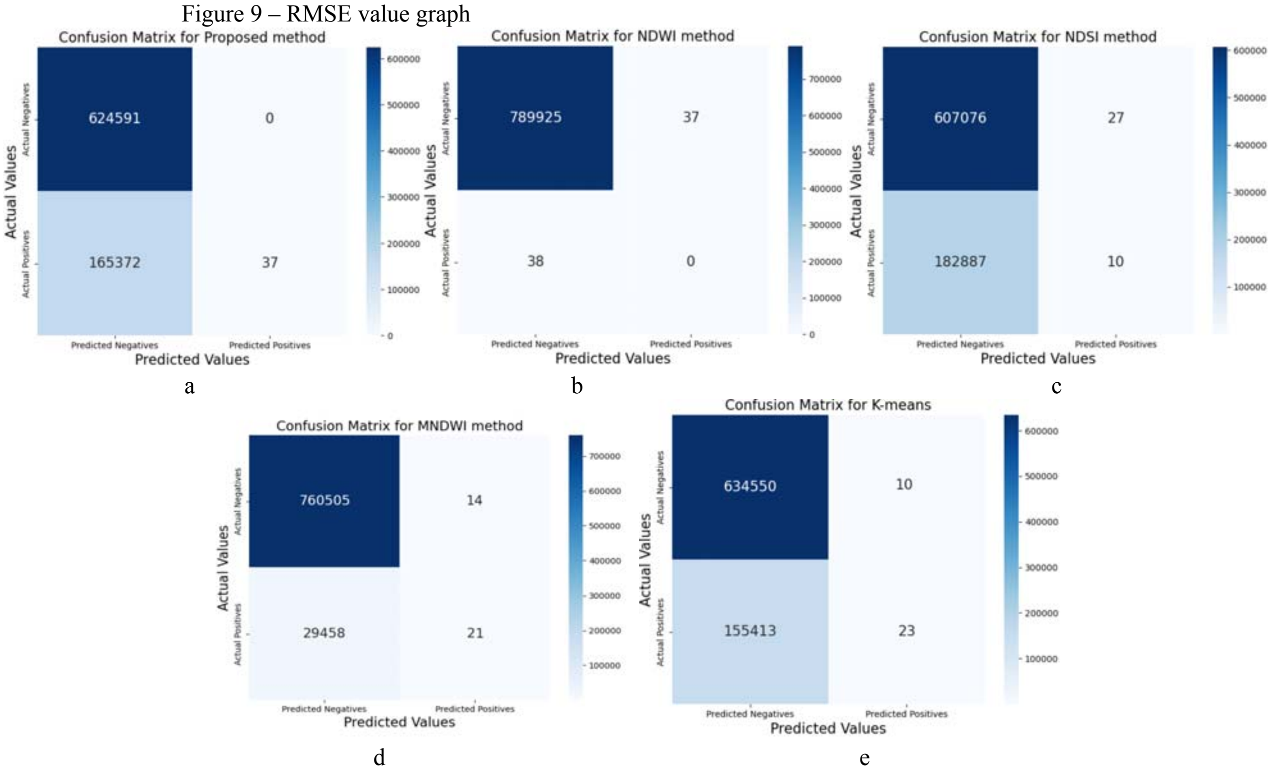

Figure 11 – Confusion matrix result for: a – proposed method; b – NDWI; c – NDSI; d – MNDWI; e – K-means

DOI 10.15588/1607-3274-2024-1-11

6 DISCUSSION

Analyzing the data in Fig. 7 on the area of the Molochny Lyman during the years 2017-2023, it is possible to make several conclusions. Firstly, the water area tends to in-crease during the analyzed years, especially from 2019 to 2020. Secondly, from 2017 to 2018, the relative change in water is positive, which may indicate an increase in water area in 2018. From 2018 to 2019, there is a decrease in the water area (negative relative change), and from 2019 to 2020 year there is a sharp increase in the water area (positive relative change); from 2020 to 2021, there is a decrease in the water area again. Various factors, including climatic conditions, anthropogenic activities, and hydrological changes, can influence changes in the area of a water body. Analyzing the dynamics of the water area of the Molochny Lyman, a significant increase was observed in 2020. This effect may be due to special climatic conditions, changes in the water supply regime, or other natural factors.

During the information verification, it was found that in 2019, large-scale measures were taken to restore the relationship between the Molochnyi Lyman and the Sea of Azov. In particular, on December 27, 2019, the estuary began to be filled with seawater, which led to a rise in water level and a decrease in water salinity in some places to 25 ppm. These actions have become a significant factor that may affect the water area in the estuary and its ecosystem in the future.

The results of Table 1 demonstrate the high accuracy of the proposed information technology compared to existing methods, emphasizing its effectiveness for recognizing and monitoring water bodies based on satellite images.

In 2023, the obtained RMSE results for different methods indicate the accuracy and differences in their effectiveness. The low RMSE value (11.35) indicates the high accuracy of the proposed method compared to the actual data for 2023. The RMSE value for the NDSI method (202.80) indicates a difference between the predicted and actual values. This indicates the low accuracy of this method.

The resulting PDF highlights that the pixel values corresponding to the 'land' class are concentrated around positive values. The pixels representing the 'water' class have negative values. The Otsu algorithm is used to determine the threshold between the 'land' and 'water' classes. This algorithm maximizes the inter-class variance between the 'land' and 'water' distributions by pre-excluding pixels that belong to the 'water' and 'other land features' classes. This approach helps to effectively determine the threshold for classifying the coastal zone in the image.

Analyzing the results confusion matrix for the proposed method and comparing it with the others, it is noticeable that the proposed method and K-means are more effective, having fewer false classifications and a significant number of correctly classified pixels as water or land. It indicates the high accuracy and reliability of the proposed method in identifying water and land regions in images.

DOI 10.15588/1607-3274-2024-1-11

CONCLUSIONS

The developed technology for automatic delineation of water bodies effectively addresses the challenges of precise and timely determination of the dynamics of water surfaces in digital optical satellite imagery. Compared to traditional methods requiring substantial effort and time for processing and analyzing large datasets, the proposed technology employs machine learning and image analysis methods to automatically extraction water bodies. It accelerates and enhances the accuracy of the monitoring process, reducing resource expenditures for data processing and interpretation.

The scientific novelty of the developed technology is to improve the methods of identifying and monitoring water bodies based on digital optical satellite images using machine learning. To use of modern algorithms and deep learning models allows for achieving high accuracy and sub-pixel resolution in the classification of surface water bodies. The developed approach demonstrates efficiency in comparison with traditional methods such as water indices and K-means, ensuring the stability of results even under variable research conditions. The obtained high accuracy and stability indicators, as a high Kappa coefficient, confirm the advantages and prospects of the developed method for application in the area of urban ecosystems and water management. This approach opens up new opportunities for more accurate and automated analysis of water bodies, contributing to the further development of research in the area of urban geographic information systems and environmental monitoring.

The proposed technology holds **practical significance** as it enables systematic monitoring of water resources and their changes in urban ecosystems. It makes it possible to accurately determine the volume of water bodies, monitor their changes over time, and predict possible environmental challenges.

Prospects for further research involve exploring seasonality and enhancing robustness in the water surface mapping.

ACKNOWLEDGEMENTS

The work is supported by the state budget scientific research project of Dnipro University of Technology "Models and information technologies of data processing and analysis in complex computer systems and networks" (state registration number 0121U114523).

REFERENCES

1. Xiang X., Li Q., Khan S., Khalaf O. Urban water resource management for sustainable environment planning using artificial intelligence techniques, *Environmental Impact Assessment Review,* 2021, Vol. 86, pp. 106515. DOI: 10.1016/j.eiar.2020.106515.
2. Bierbaum R. Leonard S., Rejeski D., Whaley C.r., Barra R., Libre C. Novel entities and technologies: Environmental benefits and risks, *Environmental Science & Policy,* 2020, Vol. 105, pp. 134–143. DOI: 10.1016/j.envsci.2019.11.002.
3. Ivanov D., Hnatushenko V., Kashtan V., Garkusha I. Computer modeling of territory flooding in the event of an emergency at Serednіodniprovska Hydroelectric Power Plant,

Naukovyi Visnyk Natsionalnoho Hirnychoho Universytetu, 2022, № 6, pp. 158–163. DOI:10.33271/nvngu/2022-6/123.
4. Mozgovoy D., Hnatushenko V., Vasyliev V. Automated recognition of vegetation and water bodies on the territory of megacities in satellite images of visible and IR bands, *ISPRS Ann. Photogramm. Remote Sens. Spatial Inf. Sci.*, 2018, IV-3, pp. 167–172. DOI: 10.5194/isprs-annals-IV-3-167-2018.
5. Xie H., Luo X., Xu X., Pan H., Tong X. Automated Subpixel Surface Water Mapping from Heterogeneous Urban Environments Using Landsat 8 OLI Imagery, *Remote Sens,* 2016, No. 8(7), P. 584. DOI:10.3390/rs8070584.
6. Ruppen D., Runnalls J., Tshimanga R., Wehrli B., Odermatt D. Optical remote sensing of large-scale water pollution in Angola and DR Congo caused by the Catoca mine tailings spill, *International Journal of Applied Earth Observation and Geoinformation*, 2023, Vol. 118, P. 103237. DOI: 10.1016/j.jag.2023.103237.
7. Palomar-Vázquez J., Pardo-Pascual J., Almonacid-Caballer J., Cabezas-Rabadán C. Shoreline Analysis and Extraction Tool (SAET): A New Tool for the Automatic Extraction of Satellite-Derived Shorelines with Subpixel Accuracy, *Remote Sensing*, 2023, No. 15(12), P. 3198. DOI: 10.3390/rs15123198.
8. Zhiwei Li. and Shen, Huanfeng and Weng, Qihao and Zhang, Yuzhuo and Dou, Peng and Zhang Cloud and cloud shadow detection for optical satellite imagery: Features, algorithms, validation, and prospects, *ISPRS Journal of Photogrammetry and Remote Sensing,* 2022, No. 188, pp. 89–108. DOI: 10.1016/j.isprsjprs.2022.03.020.
9. Mao T., Fan Y., Zhi S., Tang J. A Morphological Feature-Oriented Algorithm for Extracting Impervious Surface Areas Obscured by Vegetation in Collaboration with OSM Road Networks in Urban Areas, *A Remote Sensing*, 2022, No. 14(10), P. 2493. DOI: 10.3390/rs14102493.
10. Nardini A., Salas F., Carrasco Z., Valenzuela N., Rojas R., Vargas-Baecheler J., Yépez S. Automatic River Planform Recognition Tested on Chilean Rivers, *Water,* 2023, No. 15(14), P. 2539. DOI: 10.3390/w15142539.
11. Wenbo Li. Ying Qin, Youqiang Sun, Huang He, Ling Feng, Tian Liqiao, Ding Yulin Estimating the relationship between dam water level and surface water area for the Danjiangkou Reservoir using Landsat remote sensing images, *Remote Sensing Letters,* 2016, Vol. 7, pp. 121–130. DOI: 10.1080/2150704X.2015.1117151.
12. Xie H., Luo X., Xu X., Pan H., Tong X. Automated Subpixel Surface Water Mapping from Heterogeneous Urban Environments Using Landsat 8 OLI Imagery, *Remote Sensing,* 2016, No. 8(7), P. 584. DOI: 10.3390/rs8070584.
13. Fisher A., Flood N., Danaher T. Comparing Landsat water index methods for automated water classification in eastern Australia, *Remote Sensing of Environment,* 2016, Vol. 175, pp. 167–182. DOI: 10.1016/j.rse.2015.12.055.
14. Wangchuk S., Bolch T. Mapping of glacial lakes using Sentinel-1 and Sentinel-2 data and a random forest classifier: Strengths and challenges, *Science of Remote Sensing*, 2020, Vol. 2, P. 100008. DOI: 10.1016/j.srs.2020.100008.
15. Liu Q., Huang C., Shi Z., Zhang S. Probabilistic River Water Mapping from Landsat-8 Using the Support Vector Machine Method, *Remote Sensing*, 2020, No. 12(9), P. 1374. DOI: 10.3390/rs12091374.
16. Chatufale A., Abhishek P. Extraction of Waterbody Using Object-Based Image Analysis and XGBoost, *Advanced Machine Intelligence and Signal Processing. Singapore: Springer Nature Singapore*, 2022, pp. 341–350. DOI:10.1007/978-981-19-0840-8_25.
17. Feng W., Haigang H., Weiming X., Chuan A., Kaiqiang An. Water Body Extraction From Very High-Resolution Remote Sensing Imagery Using Deep U-Net and a Superpixel-Based Conditional Random Field Model, *IEEE Geoscience and Remote Sensing Letters,* 2018, pp. 1–5. DOI: 10.1109/LGRS.2018.2879492.
18. Jiang W., He G., Long T., Ni Y., Liu H., Peng Y., Lv K., Wang G. Multilayer Perceptron Neural Network for Surface Water Extraction in Landsat 8 OLI Satellite Images, *Remote Sensing*, 2018, No. 10 (5), P. 755. DOI: 10.3390/rs10050755.
19. Lu Li, Bing W., Shichao W., Li Fan, Qingjie L. Water Body Extraction from High-resolution Remote Sensing images Based on Scaling EfficientNets, *Journal of Physics: Conference Series,* 2021, pp. 1–5. DOI: 10.1088/1742-6596/1894/1/012100.
20. Hachiya H., Nagayoshi K., Iwaki A., Maeda T., Ueda N., Fujiwara H. Position-dependent partial convolutions for supervised spatial interpolation, *Machine Learning with Applications*, 2023, Vol. 14. DOI: 10.1016/j.mlwa.2023.100514.
21. Agarap A. Deep learning using rectified linear units (relu), 2018. DOI: 10.48550/arXiv.1803.08375.
22. Yang X., Zhao S., Qin X., Zhao N., Liang L. Mapping of Urban Surface Water Bodies from Sentinel-2 MSI Imagery at 10 m Resolution via NDWI-Based Image Sharpening, Remote Sensing, 2017, No. 9 (6), P. 596. DOI: 10.3390/rs9060596.
23. Kashtan V., Hnatushenko V., Zhir S. Information Technology Analysis of Satellite Data for Land Irrigation Monitoring, *2021 IEEE International Conference on Information and Telecommunication Technologies and Radio Electronics (UkrMiCo)*. Kyiv, Ukraine, November 29 – December 3, 2021, pp. 12–15. DOI: 10.1109/UkrMiCo52950.2021.9716592.
24. Kashtan V., Hnatushenko V. Automated pansharpening information technology of satellite images, Radio Electronics, Computer Science, Control, 2021, №2 (57), pp. 123–133. DOI: 10.15588/1607-3274-2021-2-13.
25. Sajib A., Diganta Mir T., Rahman A., Dabrowski T., Olbert A., Uddin M. Developing a novel tool for assessing the groundwater incorporating water quality index and machine learning approach, *Groundwater for Sustainable Development*, 2023, Vol. 23. DOI: 10.1016/j.gsd.2023.101049.

Received 26.12.2023.
Accepted 31.01.2024.

УДК 004.93

МАШИННЕ НАВЧАННЯ ДЛЯ АВТОМАТИЧНОГО ВИДІЛЕННЯ ВОДНИХ ОБ'ЄКТІВ ЗА ЗНІМКАМИ SENTINEL-2

Каштан В. Ю. – кан. техн. наук, доцент, доцент кафедри інформаційних технологій та комп'ютерної інженерії, Національний технічний університет «Дніпровська політехніка», Дніпро, Україна.

DOI 10.15588/1607-3274-2024-1-11

Гнатушенко В. В. – д-р техн. наук, професор, завідувач кафедри інформаційних технологій та комп'ютерної інженерії, Національний технічний університет «Дніпровська політехніка», Дніпро, Україна.

АНОТАЦІЯ

Актуальність. Враховуючи загострення екологічних та водних проблем, виникає необхідність у вдосконаленні автоматизованих методів визначення та моніторингу водних об'єктів у міських екосистемах. З врахуванням великого обсягу даних, отриманих від супутникових систем, проблема ефективного та автоматизованого вилучення водних об'єктів стає актуальною. Об'єктом дослідження є водні об'єкти, які автоматично виділяються з оптичних космічних знімків Sentinel-2 за допомогою методів машинного навчання.

Мета роботи – підвищення ефективності процесу виділення границь водних об'єктів на цифрових оптичних космічних знімках за допомогою використання методів машинного навчання.

Метод. Запропоновано автоматизовану інформаційну технологію виділення границь водних об'єктів на цифрових оптичних супутникових знімках Sentinel-2. Процес включає вісім етапів, починаючи з завантаження даних та використання топографічних карт для отримання базової інформації про предметну область. Після цього відбувається попередня обробка даних, включаючи калібрування зображень, видалення атмосферного шуму та підвищення контрастності. Далі застосовується архітектура EfficientNet-B0 для ідентифікації водних об'єктів, сприяючи оптимальному масштабуванню ширини мережі, глибини та роздільної здатності зображення. Використані ResNet блоки для стиснення та розширення каналів, що дозволяє оптимальне з'єднання великомасштабних та багатоканальних зв'язків у шарах. Після цього Regional Proposal Network визначає області інтересу (ROI), а ROI alignment забезпечує однорідність даних. Застосування Fully connected layer допомагає в сегментації областей, а Fully connected network створює бінарні маски для точної ідентифікації водних об'єктів. Заключним етапом методу є аналіз просторових та часових змін на зображеннях для виявлення різниць, змін та тенденцій, що можуть свідчити про конкретні явища чи події. Такий підхід дозволяє автоматизувати та точно визначати водні об'єкти на супутникових знімках з використанням машинного навчання.

Результати. Розроблено програмне забезпечення мовою Python, що реалізує запропонований підхід. Оцінка точності технології, проведена шляхом порівняльного аналізу з існуючими методами, такими як водні індекси та K-means, підтверджує високий рівень точності в період з 2017 по 2023 роки (досягає 98%). Коефіцієнт Каппа, який враховує ступінь узгодженості між реальною та передбачуваною класифікацією, підтверджує стабільність та достовірність нашого підходу, досягаючи значення 0.96.

Висновки. Проведені експерименти підтверджують ефективність запропонованої автоматизованої інформаційної технології та дозволяють рекомендувати її для використання в дослідженнях змін на прибережних територіях, прийняття рішень у сфері управління прибережними ресурсами та земельним використанням. Перспективи подальших досліджень можуть включати створення нових методів, які враховують сезонні зміни та забезпечують робастність при виділенні та картографуванні водних поверхонь.

КЛЮЧОВІ СЛОВА: виділення, водні об'єкти, оптичні супутникові знімки, водні індекси, машинне навчання, коефіцієнт Каппа, коефіцієнт Пірсона, матриця помилок.

ЛІТЕРАТУРА

1. Xiang X. Urban water resource management for sustainable environment planning using artificial intelligence techniques / X. Xiang, Q. Li, S. Khan, O. Khalaf // Environmental Impact Assessment Review, 2021. – Vol. 86, P. 106515. DOI: 10.1016/j.eiar.2020.106515.
2. Novel entities and technologies: Environmental benefits and risks / [R. Bierbaum, S. Leonard, D. Rejeski et al.] // Environmental Science & Policy. – 2020. – Vol. 105. – P. 134–143. DOI: 10.1016/j.envsci.2019.11.002.
3. Computer modeling of territory flooding in the event of an emergency at Seredniodniprovska Hydroelectric Power Plant / [D. Ivanov, V. Hnatushenko, V. Kashtan, I. Garkusha] // Naukovyi Visnyk Natsionalnoho Hirnychoho Universytetu. – 2022. – № 6. – P. 158–163. DOI:10.33271/nvngu/2022-6/123.
4. Mozgovoy D. Automated recognition of vegetation and water bodies on the territory of megacities in satellite images of visible and IR bands / D. Mozgovoy, V. Hnatushenko, V. Vasyliev // ISPRS Ann. Photogramm. Remote Sens. Spatial Inf. Sci. – 2018. – IV-3. – P. 167–172, DOI: 10.5194/isprs-annals-IV-3-167-2018.
5. Xie H. Automated Subpixel Surface Water Mapping from Heterogeneous Urban Environments Using Landsat 8 OLI Imagery / [H. Xie, X. Luo, X. Xu et al.] // Remote Sens. – 2016. – No. 8(7). – P. 584. DOI:10.3390/rs8070584.
6. Optical remote sensing of large-scale water pollution in Angola and DR Congo caused by the Catoca mine tailings spill / [D. Ruppen, J. Runnalls, R. Tshimanga et al.] // International Journal of Applied Earth Observation and Geoinformation. – 2023. – Vol. 118. – P. 103237. DOI: 10.1016/j.jag.2023.103237.
7. Shoreline Analysis and Extraction Tool (SAET): A New Tool for the Automatic Extraction of Satellite-Derived Shorelines with Subpixel Accuracy / [J. Palomar-Vázquez, J. Pardo-Pascual, J. Almonacid-Caballer, C. Cabezas-Rabadán] // Remote Sensing. – 2023. – No. 15(12). – P. 3198. DOI: 10.3390/rs15123198.
8. Cloud and cloud shadow detection for optical satellite imagery: Features, algorithms, validation, and prospects / [Li Zhiwei and Shen, Huanfeng and Weng, Qihao and Zhang, Yuzhuo and Dou, Peng and Zhang] // ISPRS Journal of Photogrammetry and Remote Sensing. – 2022. – No. 188. – P. 89–108. DOI: 10.1016/j.isprsjprs.2022.03.020.
9. A Morphological Feature-Oriented Algorithm for Extracting Impervious Surface Areas Obscured by Vegetation in Collaboration with OSM Road Networks in Urban Areas / [T. Mao, Y. Fan, S. Zhi, J. Tang] // A Remote Sensing. – 2022. – No. 14(10). – P. 2493. DOI: 10.3390/rs14102493.
10. Automatic River Planform Recognition Tested on Chilean Rivers / [A. Nardini, F. Salas, Z. Carrasco et al.] // Water. – 2023. – No. 15(14). – P. 2539. DOI: 10.3390/w15142539.
11. Estimating the relationship between dam water level and surface water area for the Danjiangkou Reservoir using Landsat remote sensing images / [Li Wenbo, Qin Ying, Sun Youqiang et al.] // Remote Sensing Letters. – 2016. – Vol. 7. P. 121–130. DOI: 10.1080/2150704X.2015.1117151.

DOI 10.15588/1607-3274-2024-1-11

12. Automated Subpixel Surface Water Mapping from Heterogeneous Urban Environments Using Landsat 8 OLI Imagery / [H. Xie, X. Luo, X. Xu et al.] // Remote Sensing. – 2016. – No. 8(7). – P. 584. DOI: 10.3390/rs8070584.
13. Fisher A. Comparing Landsat water index methods for automated water classification in eastern Australia // A. Fisher, N. Flood, T. Danaher // Remote Sensing of Environment. – 2016. – Vol. 175. – P. 167–182. DOI: 10.1016/j.rse.2015.12.055.
14. Wangchuk S. Mapping of glacial lakes using Sentinel-1 and Sentinel-2 data and a random forest classifier: Strengths and challenges / S. Wangchuk, T. Bolch // Science of Remote Sensing. – 2020. – Vol. 2. – P. 100008. DOI: 10.1016/j.srs.2020.100008.
15. Liu Q. Probabilistic River Water Mapping from Landsat-8 Using the Support Vector Machine Method / [Q. Liu, C. Huang, Z. Shi, S. Zhang] // Remote Sensing. – 2020. – No. 12(9). P. 1374. DOI: 10.3390/rs12091374.
16. Chatufale A. Extraction of Waterbody Using Object-Based Image Analysis and XGBoost / A. Chatufale, P. Abhishek // Advanced Machine Intelligence and Signal Processing. Singapore: Springer Nature Singapore – 2022. – P. 341–350. DOI:10.1007/978-981-19-0840-8_25.
17. Water Body Extraction From Very High-Resolution Remote Sensing Imagery Using Deep U-Net and a Superpixel-Based Conditional Random Field Model / [W. Feng, H. Haigang, X. Weiming et al.] // IEEE Geoscience and Remote Sensing Letters. – 2018. – P. 1–5. DOI: 10.1109/LGRS.2018.2879492.
18. Jiang W. Multilayer Perceptron Neural Network for Surface Water Extraction in Landsat 8 OLI Satellite Images / [W. Jiang, G. He, T. Long et al.] // Remote Sensing. – 2018. – No. 10(5). P. 755. DOI: 10.3390/rs10050755.
19. Lu Li. Water Body Extraction from High-resolution Remote Sensing images Based on Scaling EfficientNets / Li Lu, W. Bing, W. Shichao et al.] // Journal of Physics: Conference Series. – 2021. – P. 1–5. DOI: 10.1088/1742-6596/1894/1/012100.
20. Position-dependent partial convolutions for supervised spatial interpolation / [H. Hachiya, K. Nagayoshi, A. Iwaki et al.] // Machine Learning with Applications. – 2023. – Vol. 14. DOI: 10.1016/j.mlwa.2023.100514.
21. Agarap A. Deep learning using rectified linear units (relu) / A. Agarap. – 2018. DOI: 10.48550/arXiv.1803.08375.
22. Mapping of Urban Surface Water Bodies from Sentinel-2 MSI Imagery at 10 m Resolution via NDWI-Based Image Sharpening / [X. Yang, S. Zhao, X. Qin et al.] // Remote Sensing. – 2017. – No. 9 (6). – P. 596. DOI: 10.3390/rs9060596.
23. Kashtan V. Information Technology Analysis of Satellite Data for Land Irrigation Monitoring / V. Kashtan, V. Hnatushenko, S. Zhir // 2021 IEEE International Conference on Information and Telecommunication Technologies and Radio Electronics (UkrMiCo), Kyiv, Ukraine, November 29 – December 3. – 2021. – P. 12–15. DOI: 10.1109/UkrMiCo52950.2021.9716592.
24. Kashtan V. Automated pansharpening information technology of satellite images / V. Kashtan, V. Hnatushenko // Radio Electronics, Computer Science, Control. – 2021. – №2 (57). – P. 123–133. DOI: 10.15588/1607-3274-2021-2-13.
25. Sajib A. Developing a novel tool for assessing the groundwater incorporating water quality index and machine learning approach / [A. Sajib, Mir T.Diganta, A. Rahman et al.], // Groundwater for Sustainable Development. – 2023. – Vol. 23. DOI: 10.1016/j.gsd.2023.101049.

DOI 10.15588/1607-3274-2024-1-11